

Resolving the polarization puzzles in $D^0 \rightarrow VV$ Ye Cao,^{*} Yin Cheng[†], and Qiang Zhao[‡]*Institute of High Energy Physics, Chinese Academy of Sciences, Beijing 100049, People's Republic of China
and University of Chinese Academy of Sciences, Beijing 100049, People's Republic of China*

(Received 20 March 2023; accepted 7 March 2024; published 5 April 2024)

We carry out a systematic analysis of the Cabibbo-favored and singly-Cabibbo-suppressed decays of $D^0 \rightarrow VV$, and demonstrate that the long-distance mechanism due to the final-state interactions can provide a natural explanation for these mysterious polarization puzzles observed in $D^0 \rightarrow VV$ in experiments. More observables, which can be measured at BESIII, and possibly at LHCb, are also suggested.

DOI: [10.1103/PhysRevD.109.073002](https://doi.org/10.1103/PhysRevD.109.073002)

I. INTRODUCTION

In the past two decades, “polarization puzzles” arose from the decays of heavy mesons into two vectors. In the beauty sector, naive power counting predicts that $B \rightarrow VV$ ($V = \phi, K^*, \rho$, and ω) decays are dominated by the longitudinal polarization since the transverse polarization amplitudes suffer from the helicity-flipping suppression at the order of Λ_{QCD}/m_b . This prediction is confirmed in $B^0 \rightarrow \rho^+\rho^-$, $B^+ \rightarrow \rho^0\rho^+$, and $\rho^0 K^{*+}$ [1–3], which has indicated the helicity conservation [4–6] in $B \rightarrow VV$. However, apparent deviations were found in $B \rightarrow \phi K^*$, where the longitudinal polarization only accounts for about 50% of the decay rate [1,7].

In the charm sector, the situation is more complicated since the heavy quark expansion method becomes unreliable here. Although different phenomenological approaches and techniques have been developed in the literature, such as the flavor SU(3) symmetry model [8], broken flavor SU(3) symmetry model [9], pole-dominance model [10], factorization approach [8,11–14], and the heavy quark effective Lagrangian and chiral perturbation theory [15], and they describe well some of the $D \rightarrow VV$ decay channels, a systematic and coherent study of all the Cabibbo-favored (CF) and singly-Cabibbo-suppressed (SCS) decays is still unavailable.

The naive factorization model [16] and the Lorentz invariant-based symmetry model [17] indeed predict that the longitudinal polarization fraction (defined as f_L) may

not be dominant in $D \rightarrow VV$. However, the predictions seem to have quantitatively deviated from the experimental measurements. Meanwhile, experimental measurements reveal unexpected puzzling results that cannot be explained by theory. For instance, the MARK-III measurement of $D^0 \rightarrow \bar{K}^{*0}\rho^0$ shows the dominance of the transverse polarization [18], though it suffers from a large uncertainty. In contrast, the precise measurement of $D^0 \rightarrow \rho^0\rho^0$ by the FOCUS Collaboration shows large longitudinal polarization fractions of $f_L = (71 \pm 4 \pm 2)\%$ [19]. Recently, the angular distribution of $D^0 \rightarrow \omega\phi$ has been measured by the BESIII Collaboration. It is stunning to find that the final states ω and ϕ seem to be fully transversely polarized with $f_L = 0.00 \pm 0.10 \pm 0.08$, which corresponds to $f_L < 0.24$ at 95% confidence level [20]. In contrast, the partial-wave measurement by CLEO-c [21] shows that the decay of $D^0 \rightarrow \phi\rho^0$ is dominated by the S wave with $\text{BR}(D^0 \rightarrow (\phi\rho^0)_{S\text{-wave}}) = (1.40 \pm 0.12) \times 10^{-3}$. The total branching ratio $\text{BR}(D^0 \rightarrow (\phi\omega) \simeq \text{BR}(D^0 \rightarrow (\phi\omega)_T) = (0.65 \pm 0.10) \times 10^{-3}$ from BESIII [20] turns out to be much smaller than that of $D^0 \rightarrow \phi\rho^0$ from CLEO-c, i.e., $\text{BR}(D^0 \rightarrow \phi\rho^0) = (1.56 \pm 0.13) \times 10^{-3}$ [21]. Such a significant difference is also confirmed by LHCb [22]. These puzzling observations show that, although the decay of $D^0 \rightarrow VV$ has been one of the broadly studied processes, we still lack of knowledge about some crucial pieces of dynamics in its decay mechanisms.

In this work, apart from the leading short-distance mechanisms, i.e., the color-allowed direct emission (DE), color-suppressed (CS) internal W emission, and the color-suppressed flavor internal conversion (IC) by the W exchange between the quark and antiquark inside D^0 , we propose that the nonfactorizable final-state interactions (FSIs) as a long-distance dynamics could be a key to resolving the mysterious polarization puzzle in $D^0 \rightarrow VV$. Notice that for $D \rightarrow VV$ the threshold of VV is not far below the D meson mass. Namely, the charm quark is not

^{*} caoye@ihep.ac.cn[†] chengyin@ihep.ac.cn[‡] zhaoq@ihep.ac.cn

Published by the American Physical Society under the terms of the [Creative Commons Attribution 4.0 International license](https://creativecommons.org/licenses/by/4.0/). Further distribution of this work must maintain attribution to the author(s) and the published article's title, journal citation, and DOI. Funded by SCOAP³.

heavy enough. The presence of the near-threshold vector-meson rescatterings either in an S or P wave may introduce significant long-distance dynamics. It indicates the necessity for a proper treatment of the nonfactorizable FSI in $D \rightarrow VV$. It thus motivates us to carry out a systematic and coherent investigation of $D^0 \rightarrow VV$ with the long-distance FSI taken into account.

As follows, we first analyze the leading short-distance mechanisms where the DE and CS couplings will be calculated in a nonrelativistic constituent quark model (NRCQM). An effective Lagrangian approach will be adopted for deriving the FSI transition amplitudes. We introduce the FSI to those CF and SCS exclusive VV channels. Numerical results and discussions will be presented in the end with a brief summary.

II. FRAMEWORK

With the kinematic constraint, D^0 can access 14 VV decay channels, i.e., three CF channels: $K^{*-}\rho^+$, $\bar{K}^{*0}\rho^0$, $\bar{K}^{*0}\omega$; eight SCS channels: $K^{*+}K^{*-}$, $K^{*0}\bar{K}^{*0}$, $\rho^+\rho^-$, $\rho^0\rho^0$, $\omega\omega$, $\rho^0\omega$, $\rho^0\phi$, $\omega\phi$; and three doubly-Cabibbo-suppressed channels: $K^{*+}\rho^-$, $K^{*0}\rho^0$, $K^{*0}\omega$. To quantify the transition mechanisms, we distinguish between the short-distance dynamics for the quark-level transitions in the quark model and the long-distance dynamics arising from the hadronic-level interactions.

A. Short-distance mechanisms in the quark model

The typical leading order transition mechanisms via the DE, CS, and IC processes are illustrated in Figs. 1(a)–1(d), respectively. Apart from the weak coupling strengths, these three processes correspond to three topologically distinguishable amplitudes from the short-distance dynamics. In the SU(3) flavor symmetry limit and given the dominance of the short-distance dynamics, all the $D^0 \rightarrow VV$ decays can be described by linear combinations of these three leading amplitudes.

1. $1 \rightarrow 3$ transitions in the quark model

The DE and CS transitions involve the process of “ $1 \rightarrow 3$ ” decays of the initial charm quark. Their corresponding coupling strengths $g_{\text{DE}}^{(P)}$ and $g_{\text{CS}}^{(P)}$ are defined by the transition matrix element as follows:

$$\begin{aligned} i\mathcal{M}_{\text{DE/CS}}^{(P)} &= \langle V_1(\mathbf{P}_1; J_1, J_{1z}) V_2(\mathbf{P}_2; J_2, J_{2z}) | \hat{H}_{W,1 \rightarrow 3}^{(P)} | \\ &\quad \times D^0(\mathbf{P}_D; J_i, J_{iz}) \rangle \\ &\equiv g_{\text{DE/CS}}^{(P); J_{1z}; J_{2z}} V_{cq} V_{uq}, \end{aligned} \quad (1)$$

where $\mathbf{P}_1 = \mathbf{p}_1 + \mathbf{p}'_2$ and $\mathbf{P}_2 = \mathbf{p}_3 + \mathbf{p}_4$ are the momentum conservation relations for the DE transition, and $\mathbf{P}_1 = \mathbf{p}_1 + \mathbf{p}_4$ and $\mathbf{P}_2 = \mathbf{p}'_2 + \mathbf{p}_3$ are for the CS one. $\hat{H}_{W,1 \rightarrow 3}^{(P)}$ is the operator that takes different forms for the parity-violated (PV) or parity-conserved (PC) transitions and has been derived in Refs. [23–25]. The above formula contains spatial wave function integrals for which the NRCQM wave functions [26–28] are adopted. In Appendix A 1 we present the detailed expressions for the transition amplitudes of $1 \rightarrow 3$.

It can be seen that the mass differences within those VV channels will lead to different values for both $g_{\text{DE}}^{(P)}$ and $g_{\text{CS}}^{(P)}$ after taking the wave function convolutions as an additional source of the SU(3) flavor symmetry breaking.

2. $2 \rightarrow 2$ transitions in the quark model

The IC transitions involve the process of “ $2 \rightarrow 2$ ” scatterings of the initial charm and \bar{u} into the CF \bar{K}^*V channel or SCS channels. The corresponding coupling strength is defined as $g_{\text{IC}(q\bar{q})}^{(P)}$. As shown by Figs. 1(c) and 1(d), different intermediate $q\bar{q}$ poles may contribute. It implies that this mechanism involves significant SU(3) flavor symmetry breakings. From the three CF transitions of $D^0 \rightarrow \bar{K}^*V$ and the experimental data for these three channels, we see the relation $|g_{\text{DE}}^{(P)}| > |g_{\text{CS}}^{(P)}| > |g_{\text{IC}(s\bar{d})}^{(P)}|$.

The nonlocal operators for the weak and strong transitions will distinguish processes between Figs. 1(c) and 1(d). The weak matrix element and the strong matrix element are connected by the intermediate resonance state as propagators. By separately calculating the weak internal conversion and strong transition couplings, Figs. 1(c) and 1(d) together will be evaluated explicitly in the quark model, provided that the wave functions of the initial, final, and intermediate states can be described stably. In the following, we will refer to both Figs. 1(c) and 1(d) as IC processes. Intuitively, the amplitudes of these two IC processes may cancel due to the opposite sign of the real part of the propagators. Meanwhile, the IC transition deserves some attention in the D meson decays

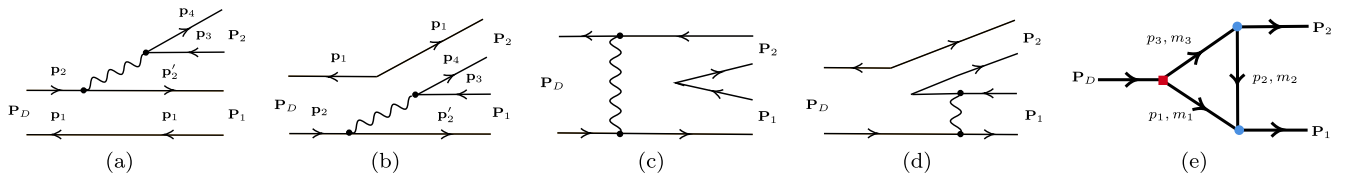


FIG. 1. Schematic diagrams for the $D^0 \rightarrow VV$ decays via the short- and long-distance transition mechanisms. (a)–(d) The short-distance transitions and stand for the DE, CS, and IC processes (c),(d), respectively; (e) illustration of the hadron-level FSI.

due to the relatively light mass of the D meson. The transition process in Fig. 1(d) is often treated as dual with Fig. 1(b). However, such a treatment should not be true, since Fig. 1(d) involves a pole structure in the transition amplitude while Fig. 1(b) does not. Moreover, we also categorize Fig. 1(c) as an IC transition since it also

involves a pole structure in the amplitude. The difference between Figs. 1(c) and Fig. 1(d) is that the weak interaction occurs before or after the strong quark-pair creation, and these two coupling vertices are connected by intermediate propagators. A general expression for the sum of Figs. 1(c) and 1(d) can be written as

$$\begin{aligned}
i\mathcal{M}_{\text{IC}}^{(\text{P})} &= \sum_{M_n(0^\pm)} \langle V_1(\mathbf{P}_1; J_{1z}) V_2(\mathbf{P}_2; J_{2z}) | \hat{H}_S | M_n(\mathbf{P}_D; J_{iz}) \rangle \frac{i}{m_D^2 - m_{M_n}^2 + im_{M_n} \Gamma_{M_n}} \langle M_n(\mathbf{P}_D; J_{iz}) | \hat{H}_{W,2 \rightarrow 2}^{(\text{P})} | D^0(\mathbf{P}_D; J_{iz}) \rangle \\
&+ \sum_{D_n^*(1^\pm)} \langle V_1(\mathbf{P}_1; J_{1z}) | H_{W,2 \rightarrow 2}^{(\text{P})} | D_n^*(\mathbf{P}_1; J_{1z}) \rangle \frac{i}{m_{V_1}^2 - m_{D_n^*}^2 + im_{D_n^*} \Gamma_{D_n^*}} \langle D_n^*(\mathbf{P}_1; J_{1z}) V_2(\mathbf{P}_2; J_{2z}) | \hat{H}_S | D^0(\mathbf{P}_D; J_{iz}) \rangle \\
&\equiv g_{\text{IC}}^{(\text{P}); J_{1z}; J_{2z}} V_{cq} V_{uq},
\end{aligned} \tag{2}$$

where cancellation between Figs. 1(c) and 1(d) is apparent. One also sees that, if the initial mass $m_D \gg m_i^{(c)}$ and $m_i^{(d)} \gg m_V$, the IC contributions will be suppressed by the propagators. Then, as expected, Fig. 1(b) will be more predominant than Figs. 1(c) and 1(d). For the case of $D^0 \rightarrow VV$, the initial D meson mass is actually not heavy enough. It means that the transition of Fig. 1(c) with the intermediate excited states may even be enhanced instead of suppressed by the propagator [29], while in Fig. 1(d) the propagator suppression is rather clear since the mass of the intermediate charmed masses is even heavier than the initial D meson. Such a situation suggests that the cancellation between Figs. 1(c) and 1(d) may not be as complete as in the case of, e.g., $B \rightarrow VV$, where the QCD factorization works better.

In Table I, we collect the short-distance amplitudes of all the CF and SCS channels. With (P) = (PC) or (PV) there are actually six quantities to account for the PC and PV transitions in each channel. It should be pointed out that, in the SU(3) flavor symmetry limit, these quantities will take the same values in all the $D^0 \rightarrow VV$ channels. However, with the consequence of the SU(3) flavor symmetry breaking, they can be different. In fact, although the DE transition is dominant, contributions from the CS and IC transitions cannot be neglected. Therefore, a more realistic evaluation of these quantities beyond the simple parametrization is necessary. Considering the complexity of $g_{\text{IC}(q\bar{q}')}^{(\text{P})}$ and its relatively small magnitudes, we leave it to be determined by the combined analysis.

One notices that an additional phase angle θ is introduced in Table I. By calculating the DE and CS in the NRCQM, these two terms can be determined with a fixed phase. θ describes the relative phase between the IC and the DE/CS amplitudes and we mention in advance that $\theta = 180^\circ$ is favored.

B. Long-distance mechanisms via the FSIs

In order to clarify the role played by the long-distance transition mechanisms, we start with the analysis of the SCS processes $D^0 \rightarrow \phi\rho^0$ and $\phi\omega$. Regarding the leading short-distance transitions, one finds that only the CS process [Fig. 1(b)] can contribute. In addition, note that ρ^0 and ω are produced by the $u\bar{u}$ component and they are degenerate in mass. These two unique features imply that given the dominance of the short-distance mechanism, these two channels should have the same decay rates. The isospin decomposition gives $u\bar{u} = \frac{1}{2}(u\bar{u} + d\bar{d}) + \frac{1}{2}(u\bar{u} - d\bar{d}) = \frac{1}{\sqrt{2}}(|\omega\rangle + |\rho^0\rangle)$, where $|\omega\rangle$ and $|\rho^0\rangle$ correspond to the flavor wave functions of ω and ρ^0 ,

TABLE I. Amplitudes of all the CF and SCS decay channels for $D^0 \rightarrow VV$ via the short-distance dynamics. The upper and lower parts are for the CF and SCS processes, respectively.

Decay channels	Amplitudes
$K^{*-}\rho^+$	$[g_{\text{DE}}^{(\text{P})} + e^{i\theta} g_{\text{IC}(s\bar{d})}^{(\text{P})}] V_{cs} V_{ud}$
$\bar{K}^{*0}\rho^0$	$\frac{1}{\sqrt{2}} [g_{\text{CS}}^{(\text{P})} - e^{i\theta} g_{\text{IC}(s\bar{d})}^{(\text{P})}] V_{cs} V_{ud}$
$\bar{K}^{*0}\omega$	$\frac{1}{\sqrt{2}} [g_{\text{CS}}^{(\text{P})} + e^{i\theta} g_{\text{IC}(s\bar{d})}^{(\text{P})}] V_{cs} V_{ud}$
$K^{*+}K^{*-}$	$[g_{\text{DE}}^{(\text{P})} + e^{i\theta} g_{\text{IC}(s\bar{s})}^{(\text{P})}] V_{cs} V_{us}$
$K^{*0}\bar{K}^{*0}$	$e^{i\theta} [g_{\text{IC}(s\bar{s})}^{(\text{P})} V_{cs} V_{us} + g_{\text{IC}(d\bar{d})}^{(\text{P})} V_{cd} V_{ud}]$
$\rho^+\rho^-$	$[g_{\text{DE}}^{(\text{P})} + e^{i\theta} g_{\text{IC}(d\bar{d})}^{(\text{P})}] V_{cd} V_{ud}$
$\rho^0\rho^0$	$\frac{1}{2} [-g_{\text{CS}}^{(\text{P})} + e^{i\theta} g_{\text{IC}(d\bar{d})}^{(\text{P})}] V_{cd} V_{ud}$
$\omega\omega$	$\frac{1}{2} [g_{\text{CS}}^{(\text{P})} + e^{i\theta} g_{\text{IC}(d\bar{d})}^{(\text{P})}] V_{cd} V_{ud}$
$\rho^0\omega$	$-\frac{1}{2} e^{i\theta} g_{\text{IC}(d\bar{d})}^{(\text{P})} V_{cd} V_{ud}$
$\phi\rho^0$	$\frac{1}{\sqrt{2}} g_{\text{CS}}^{(\text{P})} V_{cs} V_{us}$
$\phi\omega$	$\frac{1}{\sqrt{2}} g_{\text{CS}}^{(\text{P})} V_{cs} V_{us}$

respectively. Thus, the coupling strength of the CS transition for $D^0 \rightarrow \phi\rho^0$ and $D^0 \rightarrow \phi\omega$ can be expressed as

$$\begin{aligned} i\mathcal{M}_{(P)}(D^0 \rightarrow \phi\rho^0/\phi\omega) &= \langle \phi\rho^0/\phi\omega | \phi(u\bar{u}) \rangle \langle \phi(u\bar{u}) | H_{W(P)}^{(CS)} | D^0 \rangle \\ &= \frac{1}{\sqrt{2}} g_{CS}^{(P)} V_{cs} V_{us}, \end{aligned} \quad (3)$$

where (P) in the above equation can be either (PV) or (PC) denoting the amplitudes for the PV or PC transitions. It actually shows that, with the leading order approximation, these two decays should have the same decay rate and the same polarization behavior. However, the partial-wave measurement by Ref. [21] shows that the decay of $D^0 \rightarrow \phi\rho^0$ is dominated by the S wave with $\text{BR}(D^0 \rightarrow (\phi\rho^0)_{S\text{-wave}}) = (1.40 \pm 0.12) \times 10^{-3}$ and its total BR is $\text{BR}(D^0 \rightarrow \phi\rho^0) = (1.56 \pm 0.13) \times 10^{-3}$. The S wave can only come from the parity-violated transition. The relatively small P -wave contribution indicates the relatively small contributions from the parity-conserved mechanism. In contrast, the recent measurement of $D^0 \rightarrow \phi\omega$ by BESIII shows that this channel is dominated by the transverse polarization, i.e., $\text{BR}(D^0 \rightarrow (\phi\omega)_T) = (0.65 \pm 0.10) \times 10^{-3}$. Surprisingly, its BR of the longitudinally polarized decay is negligibly small. Although these two measurements involve two different observables, the suppression of the longitudinal polarization contributions and the significant difference of their total BR suggests that these two decay channels involve mechanisms beyond the leading short-distance transitions.

Recognizing that the mass of $K^*\bar{K}^*$ is almost degenerate to those of $\phi\rho^0/\phi\omega$ and the decays of $D^0 \rightarrow K^{*+}K^{*-}$ and $D^0 \rightarrow K^{*0}\bar{K}^{*0}$ actually involve different processes in Fig. 1, we anticipate that the decays of $D^0 \rightarrow \phi\rho^0$ and $D^0 \rightarrow \phi\omega$ should acquire different contributions from the intermediate $K^{*+}K^{*-}$ and $K^{*0}\bar{K}^{*0}$ rescatterings to the isovector channel $\phi\rho^0$ and isoscalar channel $\phi\omega$, respectively. Generally speaking, intermediate processes that have sizable BRs into $\phi\rho^0$ and $\phi\omega$ may contribute as long-distance mechanisms as illustrated in Fig. 1(e). However, taking into account the mass thresholds and weak coupling strengths, only some of those PP , VP , and VV channels can have sizable effects.

In Table II we list the processes that contain the DE transitions as the leading contributing channels to the FSIs and we adopt their DE couplings extracted in the NRCQM in the loop calculation. This is a reasonable approximation since they are the dominant processes for $D^0 \rightarrow VV$. The data will be fitted with all the mechanisms included. Interestingly, one sees that the intermediate PP and VP channels contribute to the VV channels differently due to the parity constraint. This allows us to extract the weak couplings from the available data for the PP and VP .

TABLE II. The weak couplings of CF and SCS channels in units of 10^{-6} which are estimated by calculating the DE process in the NRCQM, and the uncertainty comes from the model parameters for VV modes, extracted by matching the experimental data for PP and VP modes.

VV modes	BR of DE	$g_{DE}^{(PC)}$ (GeV $^{-1}$)	$g_{DE}^{(PV)}$ (GeV)
$K^{*-}\rho^+$	0.22 ± 0.06	2.61 ± 0.43	4.90 ± 0.63
$K^{*+}K^{*-}$	$(0.89 \pm 0.29)\%$	2.91 ± 0.60	5.45 ± 0.89
$\rho^+\rho^-$	$(1.33 \pm 0.49)\%$	2.96 ± 0.88	4.74 ± 0.80
<hr/>			
PP/VP modes	BR of experiment	$g^{(PC)}$	$g^{(PV)}$ (GeV)
$K^-\pi^+$	$(3.95 \pm 0.03)\%$	0	2.64 ± 0.01
K^+K^-	$(4.08 \pm 0.06) \times 10^{-3}$	0	3.84 ± 0.03
$\pi^+\pi^-$	$(1.45 \pm 0.02) \times 10^{-3}$	0	2.19 ± 0.02
$K^{*-}\pi^+$	$(6.93 \pm 1.20)\%$	1.29 ± 0.11	0
ρ^+K^-	$(11.20 \pm 0.70)\%$	1.54 ± 0.05	0
$K^{*-}K^+$	$(1.86 \pm 0.30) \times 10^{-3}$	1.16 ± 0.09	0
$K^{*+}K^-$	$(5.67 \pm 0.90) \times 10^{-3}$	2.02 ± 0.16	0
ρ^-K^+	$(5.15 \pm 0.25) \times 10^{-3}$	1.23 ± 0.03	0
$\rho^+\pi^-$	$(1.01 \pm 0.04)\%$	1.72 ± 0.03	0

In contrast, the weak couplings for $D^0 \rightarrow VV$ contain both PC and PV components.

For the decays of $D^0 \rightarrow \phi\rho^0$ and $D^0 \rightarrow \phi\omega$ we only consider the rescatterings of $D^0 \rightarrow K^{*+}K^{*-} \rightarrow \phi\rho^0$ and $\phi\omega$ as the leading long-distance amplitudes, but neglect contributions from the CS processes. Note that, although $D^0 \rightarrow K^{*+}K^{*-}$ and $\rho^+\rho^-$ are the DE processes, their experimental measurements are still unavailable. We will extract the DE amplitudes in the NRCQM as the theoretical input. For the decays of $D^0 \rightarrow VV$, the kinematics and local weak coupling operators make it a reliable estimate of the DE and CS transition amplitudes [25].

One also notices that the decays of $D^0 \rightarrow \phi\rho^0$ and $\phi\omega$ actually receive different interfering contributions from the intermediate $K^{*+}K^{*-}$ rescatterings. Namely, the DE transition can access both channels, while the IC transition only contributes to the $\phi\omega$ channel. It means that these two channels will receive different interfering contributions from the intermediate $K^{*+}K^{*-}$. To illustrate this explicitly, we write down the leading $K^{*+}K^{*-}$ rescattering amplitudes through triangle loops by exchanging \mathbb{K} (K or K^*), respectively, as follows:

$$i\mathcal{M}_{(P)\phi\rho^0}^{\text{loop}} = \frac{1}{\sqrt{2}} g_{DE}^{(P)} V_{cs} V_{us} \sum_{(\mathbb{K})} \tilde{\mathcal{I}}[(P); K^{*+}, K^{*-}, (\mathbb{K})], \quad (4)$$

$$\begin{aligned} i\mathcal{M}_{(P)\phi\omega}^{\text{loop}} &= \left(\frac{1}{\sqrt{2}} g_{DE}^{(P)} + e^{i\theta} g_{IC(s\bar{s})}^{(P)} \right) V_{cs} V_{us} \\ &\quad \times \sum_{(\mathbb{K})} \tilde{\mathcal{I}}[(P); K^{*+}, K^{*-}, (\mathbb{K})], \end{aligned} \quad (5)$$

where the sum is over the contributing meson loops $\tilde{\mathcal{I}}[(P); K^{*+}, K^{*-}, (\mathbb{K})]$; as defined before, (P) [= (PC) or (PV)] indicates the PC or PV property of the corresponding amplitude. The triangle loop function $\tilde{\mathcal{I}}$ has different integrand functions for different loops.

Taking the PC loop transition [(PC); $K^*, \bar{K}^*, (K)$] as an example, the loop integral is

$$\tilde{\mathcal{I}}[(PC); K^{*+}, K^{*-}, (K)] = \int \frac{d^4 p_1}{(2\pi)^4} V_{1\mu\nu} D^{\mu\mu'}(K^*) V_{2\mu'} D(K) V_{3\nu'} D^{\nu\nu'}(\bar{K}^*) \mathcal{F}(p_i^2), \quad (6)$$

where the vertex functions have compact forms as follows:

$$\begin{aligned} V_{1\mu\nu} &= -i\epsilon_{\alpha\beta\mu\nu} P_1^\alpha P_3^\beta, \\ V_{2\mu'} &= ig_{V_1 K^* \bar{K}} \epsilon_{\alpha\beta_1 \mu' \delta} P_1^{\alpha_1} P_{V_1}^{\beta_1} \epsilon_{V_1}^{\delta*}, \\ V_{3\nu'} &= ig_{V_2 \bar{K}^* K} \epsilon_{\alpha_2 \beta_2 \nu' \lambda} P_3^{\alpha_2} P_{V_2}^{\beta_2} \epsilon_{V_2}^{\lambda*}, \end{aligned} \quad (7)$$

with V_1 and V_2 denoting the final state ϕ and ρ^0/ω , respectively. In Eq. (6), functions $D^{\mu\mu'}(K^*) = -i(g^{\mu\mu'} - p^\mu p^{\mu'}/p^2)/(p^2 - m_{K^*}^2 + i\epsilon)$ and $D(K) = i/(p^2 - m_K^2 + i\epsilon)$ are the propagators for K^* and K , respectively, with four-vector momentum p . We note that all the vertex couplings involving the light pseudoscalar (P) and vector (V) meson couplings, i.e., g_{VPP} , g_{VVP} , and g_{VVV} , have been extracted by Refs. [30,31], such as $g_{V_1 K^* \bar{K}}$ and $g_{V_2 \bar{K}^* K}$ in Eq. (7). In Appendix A 2 the detailed integrals for the relevant loop transitions have been given.

In order to cut off the ultraviolet divergence in the loop integrals, a commonly adopted form factor is included to regularize the integrand,

$$\mathcal{F}(p_i^2) = \prod_i \left(\frac{\Lambda_i^2 - m_i^2}{\Lambda_i^2 - p_i^2} \right), \quad (8)$$

where $\Lambda_i \equiv m_i + \alpha \Lambda_{\text{QCD}}$ with m_i the mass of the i th internal particle, and $\Lambda_{\text{QCD}} = 220$ MeV with $\alpha = 1-2$ as the cutoff parameter [32].

III. RESULTS AND DISCUSSIONS

A. Fitting scheme

In our approach there are limited numbers of parameters to be fitted by the available data. Apart from the phase angle θ and cutoff parameter α , the IC couplings, i.e., $g_{\text{IC}(s\bar{d})}^{(P)}$, $g_{\text{IC}(s\bar{s})}^{(P)}$, $g_{\text{IC}(d\bar{d})}^{(P)}$, are treated as free parameters and will be determined by the overall fitting. Concerning the phase angle θ , our numerical study shows that $\theta = 180^\circ$ is favored. This indicates a natural phase between the short- and long-distance amplitudes. Namely, a sign may arise from between the quark- and hadronic-level amplitudes due to the convention adopted. Also, the results seem not to be sensitive to α within a reasonable range of values. Hence, we first restrict $\alpha = 1.4 \pm 0.14$ as an overall parameter and then fit the IC couplings to the existing experimental data.

Note that the IC coupling $g_{\text{IC}(s\bar{d})}^{(P)}$ appears in the CF modes, i.e., $D^0 \rightarrow K^{*-}\rho^+$, $\bar{K}^{*0}\rho^0$, and $\bar{K}^{*0}\omega$, while $g_{\text{IC}(s\bar{s})}^{(P)}$ and $g_{\text{IC}(d\bar{d})}^{(P)}$ appear in the SCS modes, i.e., $D^0 \rightarrow K^{*+}K^{*-}$, $K^{*0}\bar{K}^{*0}$, $\rho^+\rho^-$, $\rho^0\rho^0$, $\omega\omega$, and $\rho^0\omega$. Experimental measurements of the CF decays of $D^0 \rightarrow K^{*-}\rho^+$, $\bar{K}^{*0}\rho^0$, and $\bar{K}^{*0}\omega$ can be found in the literature [18,21,33,34]. The SCS decays of $K^{*0}\bar{K}^{*0}$ [21] and $\rho^0\rho^0$ [19,21] were also measured by experiment. However, one notices that there are quite significant differences between the results from Refs. [21,19].

To proceed, we adopt the data for $D^0 \rightarrow K^{*-}\rho^+$, $\bar{K}^{*0}\rho^0$, $\bar{K}^{*0}\omega$, and $K^{*0}\bar{K}^{*0}$ as input for the determination of the IC couplings. The fitting results for these input channels are listed in Table III as a comparison. The numerical study shows that in the SCS transitions $g_{\text{IC}(s\bar{s})}^{(\text{PC})} \simeq g_{\text{IC}(d\bar{d})}^{(\text{PC})} \simeq (1.0-1.2) \times 10^{-6} \text{ GeV}^{-1}$ and $g_{\text{IC}(s\bar{s})}^{(\text{PV})} \simeq g_{\text{IC}(d\bar{d})}^{(\text{PV})} \simeq (0.8-1.0) \times 10^{-6} \text{ GeV}$ can be determined. We also find that the coupling $g_{\text{IC}(s\bar{d})}^{(P)}$ in the CF transition is different from $g_{\text{IC}(s\bar{s})}^{(P)}$ in the SCS, i.e., $g_{\text{IC}(s\bar{d})}^{(\text{PC})} = (0.2-0.5) \times 10^{-6} \text{ GeV}^{-1}$ and $g_{\text{IC}(s\bar{d})}^{(\text{PV})} = (2.5-3.0) \times 10^{-6} \text{ GeV}$. This is understandable since these quantities describe different intermediate flavor configurations in the

TABLE III. The fitted branching ratios in comparison with the experimental data in our framework. The best fitting gives $g_{\text{IC}(s\bar{d})}^{(\text{PC})} \simeq (0.2-0.5) \times 10^{-6} \text{ GeV}^{-1}$, $g_{\text{IC}(s\bar{d})}^{(\text{PV})} \simeq (2.5-3.0) \times 10^{-6} \text{ GeV}$, $g_{\text{IC}(s\bar{s})}^{(\text{PC})} \simeq g_{\text{IC}(d\bar{d})}^{(\text{PC})} \simeq (1.0-1.2) \times 10^{-6} \text{ GeV}^{-1}$, and $g_{\text{IC}(s\bar{s})}^{(\text{PV})} \simeq g_{\text{IC}(d\bar{d})}^{(\text{PV})} \simeq (0.8-1.0) \times 10^{-6} \text{ GeV}$.

CF	Experiments	Fitted values ($\alpha = 1.4 \pm 0.14$)	SCS	Experiments	Fitted values ($\alpha = 1.4 \pm 0.14$)
$K^{*-}\rho^+$	$(6.5 \pm 2.5)\%$ [33]	$(6.58_{-0.10}^{+0.14})\%$	$K^{*0}\bar{K}^{*0}[S]$	$(5.04 \pm 0.30) \times 10^{-4}$ [21]	$(5.31_{-2.04}^{+3.02}) \times 10^{-4}$
$\bar{K}^{*0}\rho^0$	$(1.515 \pm 0.075)\%$ [34] $(1.59 \pm 0.35)\%$ [18]	$(1.53_{-0.26}^{+0.24})\%$	$K^{*0}\bar{K}^{*0}[P]$	$(2.70 \pm 0.18) \times 10^{-4}$ [21]	$(2.82_{-0.13}^{+0.08}) \times 10^{-4}$
$\bar{K}^{*0}\rho^0[T]$	$(1.8 \pm 0.6)\%$ [18]	$(1.10_{-0.16}^{+0.13})\%$	$K^{*0}\bar{K}^{*0}[D]$	$(1.06 \pm 0.09) \times 10^{-4}$ [21]	$(0.11_{-0.03}^{+0.04}) \times 10^{-4}$
$\bar{K}^{*0}\omega$	$(1.1 \pm 0.5)\%$ [33]	$(0.95_{-0.06}^{+0.04})\%$	$K^{*0}\bar{K}^{*0}(\text{Total})$	$(8.80 \pm 0.36) \times 10^{-4}$ [21]	$(8.31_{-2.24}^{+3.18}) \times 10^{-4}$

TABLE IV. The calculated polarization and partial-wave BRs of all the CF and SCS decays of $D^0 \rightarrow VV$ in units of 10^{-3} . Columns 3–10 are the results of other theoretical models, including the factorization approach [8,11–14], flavor SU(3) symmetry model (asterisk) [8], broken flavor SU(3) symmetry model [9], and pole-dominance model [10], and the values in parentheses are the results the FSIs considered. The last column lists the experimental data, while the second- and third-to-last columns list our model calculations without and with the FSIs, respectively.

Process		[13]	[12]	[14]	[11]	[8]	[8]*	[9]	[10]	Our results		Experiments
										without FSIs	Our results with FSIs	
$K^{*-}\rho^+$	T	47.59	$57.92^{+0.96}_{-0.59}$...
	L	34.7 ± 1.4	4.58	$7.88^{+0.43}_{-0.43}$...
	Total	...	113	8.0(77.2)	236	65.5(55.9)	...	59 ± 24	65	52.17	$65.80^{+1.39}_{-1.02}$	65.0 ± 25.0 [33]
$\bar{K}^{*0}\rho^0$	T	12.36	$10.95^{+1.28}_{-1.55}$	18.0 ± 6.0 [18]
	L	13.2 ± 1.3	5.31	$4.34^{+1.09}_{-1.09}$...
	Total	...	18	8.2(26.0)	22.9	7.0(16.6)	...	16 ± 4	8.5	17.68	$15.29^{+2.37}_{-2.64}$	15.9 ± 3.5 [18]
$\bar{K}^{*0}\omega$	T	7.52	$6.85^{+0.36}_{-0.51}$...
	L	34.9 ± 2.7	2.76	$2.62^{+0.09}_{-0.08}$...
	Total	...	16	10.0(12.6)	21.9	6.6(6.6)	28 ± 17	11 ± 5	7.9	10.28	$9.48^{+0.45}_{-0.59}$	11.0 ± 5.0 [33]
$K^{*+}K^{*-}$	T	4.02	$6.75^{+0.26}_{-0.38}$...
	L	1.1 ± 0.05	1.83	$3.17^{+0.09}_{-0.17}$...
	Total	...	7.3	10.0(3.3)	10.1	2.4(1.8)	1.5 ± 0.8	$2.4^{+4.1}_{-2.1}$...	5.86	$9.92^{+0.34}_{-0.55}$...
$K^{*0}\bar{K}^{*0}$	S	0.92	$0.53^{+0.30}_{-0.20}$	0.50 ± 0.03 [21]
	P	0.30	$0.28^{+0.008}_{-0.012}$	0.27 ± 0.02 [21]
	D	0.006	$0.01^{+0.004}_{-0.003}$	0.11 ± 0.01 [21]
	T	0.84	$0.58^{+0.19}_{-0.13}$...
	L	0.01 ± 0.002	0.39	$0.25^{+0.11}_{-0.08}$...
	Total	10.0(1.1)	...	0(0.6)	0.65 ± 0.3	2.0 ± 1.5	0.026	1.23	$0.83^{+0.31}_{-0.22}$	0.88 ± 0.04 [21]
$\rho^+\rho^-$	T	5.44	$5.80^{+0.36}_{-0.36}$...
	L	3.2 ± 0.1	1.36	$3.22^{+0.004}_{-0.03}$...
	Total	...	6.6	7.3(6.2)	13.1	5.3(4.4)	5.4 ± 3.2	<15	...	6.81	$9.03^{+0.36}_{-0.34}$...
$\rho^0\rho^0$	S	...	0.85	0.49	$0.45^{+0.40}_{-0.26}$	0.18 ± 0.13 [21]
	P	...	0.091	0.23	$0.56^{+0.10}_{-0.10}$	0.53 ± 0.13 [21]
	D	...	0.034	0.01	$0.03^{+0.01}_{-0.01}$	0.62 ± 0.30 [21]
	T	0.48	$0.87^{+0.32}_{-0.25}$	0.56 ± 0.07 [19]
	L	1.1 ± 0.1	0.25	$0.18^{+0.19}_{-0.13}$	1.27 ± 0.10 [19]
	Total	...	0.97	7.3(1.6)	1.18	0.5(1.3)	1.7 ± 1.0	<6.5	...	0.73	$1.05^{+0.50}_{-0.37}$	1.85 ± 0.13 [19]
$\omega\omega$	T	0.019	$0.12^{+0.018}_{-0.017}$...
	L	0.47 ± 0.07	0.00065	$0.03^{+0.0005}_{-0.001}$...
	Total	...	0.68	...	1.08	0.2(0.2)	2.3 ± 1.4	0.020	$0.15^{+0.018}_{-0.018}$...
$\rho^0\omega$	T	0.84	$0.15^{+0.013}_{-0.002}$...
	L	0.95 ± 0.07	0.13	$0.06^{+0.004}_{-0.008}$...
	Total	0.03	...	0.02(0.02)	3.0 ± 1.8	<84	...	0.97	$0.21^{+0.009}_{-0.005}$...
$\phi\rho^0$	S	...	0.63	0.48	$1.35^{+0.23}_{-0.20}$	1.40 ± 0.12 [21]
	P	...	0.025	0.05	$0.11^{+0.04}_{-0.03}$	0.08 ± 0.04 [21]
	D	...	0.001	~ 0	$0.002^{+0.001}_{-0.001}$	0.08 ± 0.03 [21]
	T	0.37	$1.02^{+0.21}_{-0.18}$...
	L	0.65 ± 0.04	0.16	$0.45^{+0.07}_{-0.06}$...
	Total	...	0.66	7.6(0.4)	1.02	0.26(0.26)	0.038 ± 0.014	1.9 ± 0.5	0.22	0.53	$1.47^{+0.27}_{-0.24}$	1.56 ± 0.13 [21]
$\phi\omega$	T	0.34	$0.67^{+0.12}_{-0.10}$	0.65 ± 0.10 [20]
	L	1.41 ± 0.09	0.15	$0.03^{+0.001}_{-0.002}$	~ 0 [20]
	Total	...	0.66	...	0.92	0.23(0.23)	0.035 ± 0.13	0.49	$0.69^{+0.12}_{-0.10}$	0.65 ± 0.10 [20]

IC transitions that can also be associated with SU(3) flavor symmetry breaking. With these fitted quantities, we can then calculate the polarization and partial-wave BRs of all the other CF and SCS channels as the predictions of our model. In particular, a comparison with the measured channels of $D^0 \rightarrow \rho^0 \rho^0$ [19,21], $\phi \rho^0$ [21], and $\phi \omega$ [20] can serve as a test of our model.

B. Polarization and partial-wave BRs

In Table IV we present our model calculations of all the CF and SCS channels with and without the FSIs in comparison with the experimental data and other theoretical calculations that can help to clarify the role played by the long-distance mechanism.

Note that it is insufficient for disentangling the role played by the long-distance mechanism given that only the $D^0 \rightarrow \bar{K}^* V$ ($V = \rho^+, \rho^0, \omega$) channels are considered. The latter two channels can be connected by the isospin relation and the interferences between the CS and IC can account for their difference by adjusting the IC coupling parameter. However, the combined analysis can give clear evidence for the FSIs and we highlight some of the key observations below:

- (I) For $D^0 \rightarrow \phi \rho^0$ and $\phi \omega$, where the IC transition does not contribute, the FSIs can naturally explain the ordering of their total BRs and provide a cancellation mechanism for the longitudinal polarization in the $\phi \omega$ channel.

We plot the cutoff parameter α dependence of the partial-wave BRs of $D^0 \rightarrow \phi \rho^0$ in Fig. 2(a) and polarization BRs of $\phi \omega$ in Fig. 2(b), respectively, to compare with the experimental data (horizontal bands) [20,21]. The vertical lines indicate the range of α with which the experimental data can be well reproduced.

In Fig. 2(a) the dot-dashed (S wave), dashed (P wave), and dotted lines (D wave) denote the cutoff parameter α dependence of the calculated

partial-wave BRs of $D^0 \rightarrow \phi \rho^0$ in comparison with the experimental data [21] (horizontal bands). The dominance of the S wave is confirmed, which means that the transition is dominantly via the PV processes. Note that the data have quite large errors and the P -wave $[(0.08 \pm 0.04) \times 10^{-4}]$ and D -wave $[(0.08 \pm 0.03) \times 10^{-4}]$ bands almost exactly overlap with each other. Because of the large errors with the P - and D -wave data, more precise measurements are needed in the future, though it does not affect the main conclusion of the S -wave dominance. We also calculate the polarization BRs for $D^0 \rightarrow \phi \rho^0$ and the results are presented in Table IV. It shows that the transverse polarization BR is about 2 times larger than the longitudinal one. This feature is different from the observations of $D^0 \rightarrow \phi \omega$, where the longitudinal BR turns out to be much smaller than the transverse one [20].

In Fig. 2(b) the cutoff dependence of the $D^0 \rightarrow \phi \omega$ polarization BRs are shown by the dot-dashed (transverse) and dashed lines (longitudinal) in comparison with the data (horizontal band). Note that our result for the longitudinal polarization BR $(0.03_{-0.002}^{+0.001}) \times 10^{-3}$ is small enough to be accommodated by the data. In terms of the longitudinal polarization fraction f_L , we have $f_L \simeq 0.045_{-0.009}^{+0.011}$, which is consistent with the BESIII measurement, i.e., $f_L < 0.24$ at 95% confidence level [20]. We note that all the other existing calculations have predicted comparable (or equal) BRs for $D^0 \rightarrow \phi \rho^0$ and $\phi \omega$ [8–14].

- (II) A combined view of $D^0 \rightarrow \rho^0 \rho^0$, $\omega \omega$, and $\rho^0 \omega$ can be gained. As shown by Table I, the CS and IC amplitudes have a constructive phase in the $\rho^0 \rho^0$ channel, but destructive in $\omega \omega$. It thus predicts a small BR for $\omega \omega$. Significant enhancement comes from the $K^{*+} K^{*-}$ and $\rho^+ \rho^-$ rescatterings, and the numerical results in Table IV for $\omega \omega$ provide a quantitative estimate of the FSI effects in this

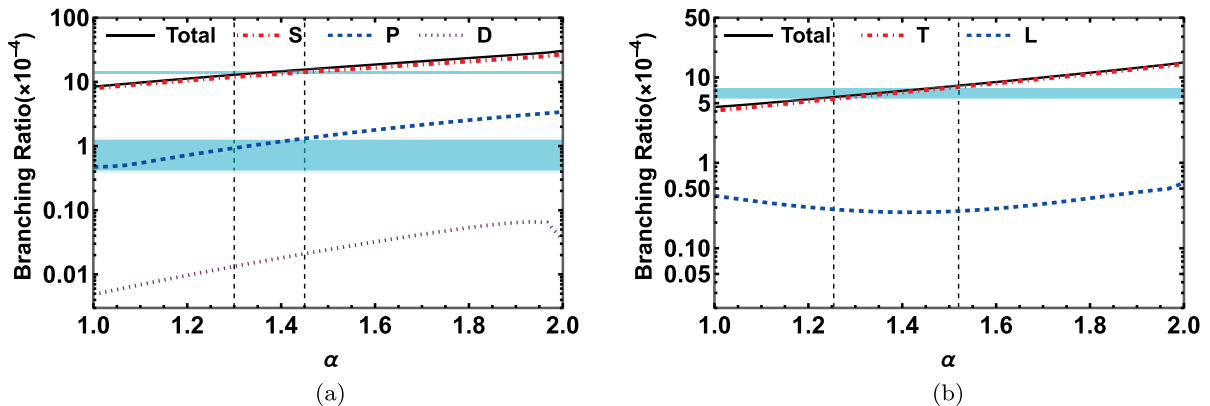


FIG. 2. Cutoff parameter α dependence of (a) the partial-wave BRs of $D^0 \rightarrow \phi \rho^0$ and (b) polarization BRs of $\phi \omega$, respectively. The solid lines stand for the total BRs. The partial-wave and polarization BRs are denoted by the line legends.

TABLE V. Input values of the constituent quark masses and harmonic oscillator strengths adopted in our calculations, which are from Refs. [26–28].

HO strength	Values (GeV)	Quark mass	Values (GeV)
R_D	0.66	m_c	1.628
R_{K^*}	0.48	m_s	0.419
$R_{\rho/\omega}$	0.45	m_q	0.22
R_ϕ	0.51

channel. An interesting feature with the $\rho^0\omega$ channel is that its CS amplitudes actually cancel out and only the IC amplitude can contribute as the leading short-distance mechanism. However, due to the destructive interference from the FSIs, its total BR is predicted to be $\sim(0.21_{-0.005}^{+0.009}) \times 10^{-3}$ which is comparable with $\rho^0\rho^0$. In comparison with other model calculations our results for $\rho^+\rho^-$, $\rho^0\rho^0$, and $\omega\omega$ are in agreement with Refs. [12], but quite different from other calculations [8–11,13,14]. Note that Ref. [12] does not calculate the $\rho^0\omega$ channel, while our prediction for $\rho^0\omega$ is very different from other existing models. Hence, a systematic measurement of these nonstrange VV channels at BESIII can provide a test of our model.

- (III) Another interesting observation about $D^0 \rightarrow VV$ is that the SCS decays of $K^{*+}K^{*-}$ and $\rho^+\rho^-$ have not been measured in experiment so far. Since they involve the DE transitions, their decay BRs are expected to be sizable and they should be among the most important decay channels for D^0 . Also, the polarization and/or partial-wave BRs of the CF channel $K^{*-}\rho^+$ are unavailable. Although theoretical estimates can be found in the literature, experimental data will provide a better constraint on the NRCQM input in our model. These channels can be accessed by the BESIII experiment and analyses of these channels are strongly recommended.

IV. SUMMARY

In this work we carry out a systematic analysis of the CF and SCS decays of $D^0 \rightarrow VV$ by taking into account the long-distance FSIs as a crucial mechanism for understanding the mysterious polarization puzzles. We show that the NRCQM provides a reasonably good description of the DE

and CS transitions with explicit phase constraints. The IC transition contains more profound effects arising from the complicated intermediate configurations. In our approach, it can be well parametrized out with the FSIs considered and can be determined by the experimental data. Our analysis shows that the stunning discrepancies of the decay rates between $D^0 \rightarrow \phi\rho^0$ and $\phi\omega$, and the unexpectedly small longitudinal polarization BR of the $\phi\omega$ channel, can be naturally explained by the FSIs. It provides clear evidence for such a long-distance mechanism in D meson decays. We also strongly recommend future precise and completed measurements of $D^0 \rightarrow VV$ at BESIII, since it will provide us a unique probe for resolving some of those profound nonperturbative dynamics.

ACKNOWLEDGMENTS

Authors would like to thank Professor Hai-Yang Cheng for useful discussions. This work is supported, in part, by the National Natural Science Foundation of China (Grant No. 12235018), DFG and NSFC funds to the Sino-German CRC 110 ‘‘Symmetries and the Emergence of Structure in QCD’’ (NSFC Grant No. 12070131001, DFG Project-ID 196253076), National Key Basic Research Program of China under Contract No. 2020YFA0406300, and Strategic Priority Research Program of Chinese Academy of Sciences (Grant No. XDB34030302).

APPENDIX: TRANSITION AMPLITUDES

There are three nonvanishing helicity amplitudes for $D^0 \rightarrow VV$: \mathcal{M}^{++} , \mathcal{M}^{--} , and \mathcal{M}^{00} , where the superscripts ‘‘ \pm ’’ and ‘‘0’’ denote the helicity of the final vector meson along the momentum direction of one of the final vector meson. The nonvanishing amplitudes \mathcal{M}^{++} and \mathcal{M}^{--} are not independent, and symmetry connects them via $\mathcal{M}_{\text{PC}}^{++} = -\mathcal{M}_{\text{PC}}^{--}$ and $\mathcal{M}_{\text{PV}}^{++} = \mathcal{M}_{\text{PV}}^{--}$. Other amplitudes $\mathcal{M}^{\pm\mp}$ and $\mathcal{M}_{\text{PC}}^{00}$ vanish.

1. Short-distance transition amplitudes extracted in the quark model

The transition amplitudes of the DE and CS processes as the short-distance dynamics are calculated in the NRCQM [26–28] and the operators have been extracted in Refs. [23–25]. The transition amplitudes for the DE and CS processes are listed below for different channels.

DE process:

$$\mathcal{M}_{\text{PC}}^{++}(D^0 \rightarrow K^{*-}\rho^+) = \frac{G_F V_{cs} V_{ud} R_D^{3/2} R_K^{3/2} R_\rho^{3/2} ((m_c + m_q)m_s R_D^2 + (m_s + m_q)m_c R_K^2) p}{2\pi^{9/4} m_c m_s (m_s + m_q) (R_D^2 + R_K^2)^{5/2}} \quad (\text{A1})$$

$$\times \exp\left(-\frac{m_q^2 p^2}{2(m_s + m_q)^2 (R_D^2 + R_K^2)}\right), \quad (\text{A2})$$

$$\mathcal{M}_{\text{PV}}^{++}(D^0 \rightarrow K^{*-}\rho^+) = \frac{G_F V_{cs} V_{ud} R_D^{3/2} R_K^{3/2} R_\rho^{3/2}}{\pi^{9/4} (R_D^2 + R_K^2)^{3/2}} \times \exp\left(-\frac{m_q^2 p^2}{2(m_s + m_q)^2 (R_D^2 + R_K^2)}\right), \quad (\text{A3})$$

$$\mathcal{M}_{\text{PV}}^{00}(D^0 \rightarrow K^{*-}\rho^+) = -\frac{G_F V_{cs} V_{ud} R_D^{3/2} R_K^{3/2} R_\rho^{3/2}}{\pi^{9/4} (R_D^2 + R_K^2)^{3/2}} \times \exp\left(-\frac{m_q^2 p^2}{2(m_s + m_q)^2 (R_D^2 + R_K^2)}\right), \quad (\text{A4})$$

$$\mathcal{M}(D^0 \rightarrow K^{*+}K^{*-}) = \mathcal{M}(D^0 \rightarrow K^{*-}\rho^+) \times [R_\rho \xrightarrow{\text{replace}} R_K, V_{ud} \xrightarrow{\text{replace}} V_{us}], \quad (\text{A5})$$

$$\mathcal{M}(D^0 \rightarrow \rho^+\rho^-) = \mathcal{M}(D^0 \rightarrow K^{*-}\rho^+) \times [R_K \xrightarrow{\text{replace}} R_\rho, m_s \xrightarrow{\text{replace}} m_q, V_{cs} \xrightarrow{\text{replace}} V_{cd}]. \quad (\text{A6})$$

CS process:

$$\mathcal{M}_{\text{PC}}^{++}(D^0 \rightarrow \bar{K}^{*0}\rho^0) = \frac{G_F V_{cs} V_{ud} (R_D R_K R_\rho)^{3/2} ((m_c + m_q) R_D^2 + 2m_c R_\rho^2) p}{12\sqrt{2}\pi^{9/4} m_c m_q (R_D^2 + R_\rho^2)^{5/2}} \exp\left(-\frac{p^2}{8(R_D^2 + R_\rho^2)}\right), \quad (\text{A7})$$

$$\mathcal{M}_{\text{PV}}^{++}(D^0 \rightarrow \bar{K}^{*0}\rho^0) = \frac{G_F V_{cs} V_{ud} (R_D R_K R_\rho)^{3/2}}{3\sqrt{2}\pi^{9/4} (R_D^2 + R_\rho^2)^{3/2}} \times \exp\left(-\frac{p^2}{8(R_D^2 + R_\rho^2)}\right), \quad (\text{A8})$$

$$\mathcal{M}_{\text{PV}}^{00}(D^0 \rightarrow \bar{K}^{*0}\rho^0) = -\frac{G_F V_{cs} V_{ud} (R_D R_K R_\rho)^{3/2}}{3\sqrt{2}\pi^{9/4} (R_D^2 + R_\rho^2)^{3/2}} \times \exp\left(-\frac{p^2}{8(R_D^2 + R_\rho^2)}\right), \quad (\text{A9})$$

$$\mathcal{M}(D^0 \rightarrow \bar{K}^{*0}\omega) = \mathcal{M}(D^0 \rightarrow \bar{K}^{*0}\rho^0) [R_\rho \xrightarrow{\text{replace}} R_\omega], \quad (\text{A10})$$

$$\mathcal{M}(D^0 \rightarrow \phi\rho^0) = \mathcal{M}(D^0 \rightarrow \bar{K}^{*0}\rho^0) \times [R_K \xrightarrow{\text{replace}} R_\phi, V_{ud} \xrightarrow{\text{replace}} V_{us}], \quad (\text{A11})$$

$$\mathcal{M}(D^0 \rightarrow \phi\omega) = \mathcal{M}(D^0 \rightarrow \bar{K}^{*0}\omega) \times [R_K \xrightarrow{\text{replace}} R_\omega, V_{ud} \xrightarrow{\text{replace}} V_{us}], \quad (\text{A12})$$

$$\mathcal{M}(D^0 \rightarrow \rho^0\rho^0) = -\frac{1}{\sqrt{2}} \mathcal{M}(D^0 \rightarrow \bar{K}^{*0}\rho^0) \times [R_K \xrightarrow{\text{replace}} R_\rho, V_{cs} \xrightarrow{\text{replace}} V_{cd}], \quad (\text{A13})$$

$$\mathcal{M}(D^0 \rightarrow \omega\omega) = \frac{1}{\sqrt{2}} \mathcal{M}(D^0 \rightarrow \bar{K}^{*0}\omega) \times [R_K \xrightarrow{\text{replace}} R_\omega, V_{cs} \xrightarrow{\text{replace}} V_{cd}]. \quad (\text{A14})$$

In the above equations, $p \equiv |\mathbf{p}|$ denotes the three-vector momentum of the final vector mesons in the initial-state rest frame; m_q is the mass of the light quarks (u, d); m_s and m_c represent the masses of the s and c quark, respectively; $R_D, R_K, R_{\omega/\rho}$, and R_ϕ are the harmonic oscillator (HO) strengths determined by the ground-state mesons $D^0, K^*, \omega/\rho^0$, and ϕ , respectively. The values adopted for these quark model parameters are from Refs. [26–28] and they are listed in Table V.

2. Long-distance transition amplitudes from FSI

In this section, we present the loop amplitudes for the convenience of tracking the calculation details. For simplicity, we do not distinguish the coupling constants at the hadronic vertices but just denote them as g_i with $i = 1, 2, 3$. The amplitudes for different processes are listed explicitly as follows, and we employ LOOPTOOLS¹ to accomplish the following numerical calculations:

¹<https://www.feynarts.de/looptools/>.

$\tilde{I}[(\text{PC}), K^*, \bar{K}^*, (K)]:$

$$\begin{aligned}
i\mathcal{M} &= g_1 g_2 g_3 \int \frac{d^4 p_1}{(2\pi)^4} \frac{\epsilon_{\alpha\beta\mu\nu} p_1^\alpha p_3^\beta (g^{\mu\mu'} - \frac{p_1^\mu p_1^{\mu'}}{p_1^2}) \epsilon_{\alpha_1\beta_1\mu_1\delta} p_1^{\alpha_1} p_{V_1}^{\beta_1} \epsilon_{V_1}^{\delta*} \epsilon_{\alpha_2\beta_2\nu_1\lambda} p_3^{\alpha_2} p_{V_2}^{\beta_2} \epsilon_{V_2}^{\lambda*} (g^{\nu\nu'} - \frac{p_3^\nu p_3^{\nu'}}{p_3^2})}{(p_1^2 - m_{K^*}^2 + i\epsilon)(p_2^2 - m_K^2 + i\epsilon)(p_3^2 - m_{K^*}^2 + i\epsilon)} \mathcal{F}(p_i^2) \\
&= g_1 g_2 g_3 \int \frac{d^4 p_1}{(2\pi)^4} \frac{\epsilon_{\alpha\beta\mu\nu} p_1^\alpha p_3^\beta \times \epsilon_{\alpha_1\beta_1\mu_1\delta} p_1^{\alpha_1} p_{V_1}^{\beta_1} \epsilon_{V_1}^{\delta*} \times \epsilon_{\alpha_2\beta_2\nu_1\lambda} p_3^{\alpha_2} p_{V_2}^{\beta_2} \epsilon_{V_2}^{\lambda*}}{(p_1^2 - m_{K^*}^2 + i\epsilon)(p_2^2 - m_K^2 + i\epsilon)(p_3^2 - m_{K^*}^2 + i\epsilon)} \mathcal{F}(p_i^2) \\
&= g_1 g_2 g_3 \int \frac{d^4 p_1}{(2\pi)^4} \frac{\mathcal{F}(p_i^2)}{(p_1^2 - m_{K^*}^2 + i\epsilon)(p_2^2 - m_K^2 + i\epsilon)(p_3^2 - m_{K^*}^2 + i\epsilon)} \\
&\quad \times \{ \epsilon_{\alpha\beta\delta\lambda} p_{V_1}^\alpha p_{V_2}^\beta \epsilon_{V_1}^{\delta*} \epsilon_{V_2}^{\lambda*} [(p_1 \cdot p_{V_1})^2 + (p_1 \cdot p_{V_1})(p_1 \cdot p_{V_2}) - p_1^2 (p_{V_1}^2 + p_{V_1} \cdot p_{V_2})] \\
&\quad + \epsilon_{\alpha\beta\delta\lambda} p_1^\alpha p_{V_2}^\beta \epsilon_{V_1}^{\delta*} \epsilon_{V_2}^{\lambda*} [p_1^2 p_{V_1}^2 - (p_1 \cdot p_{V_1})^2] + \epsilon_{\alpha\beta\delta\lambda} p_{V_1}^\alpha p_1^\beta \epsilon_{V_1}^{\delta*} \epsilon_{V_2}^{\lambda*} [-p_1^2 p_{V_2}^2 + (p_1 \cdot p_{V_2})^2] \\
&\quad + \epsilon_{\alpha\beta\delta\lambda} p_{V_1}^\alpha p_{V_2}^\beta p_1^\delta \epsilon_{V_2}^{\lambda*} [(p_1 \cdot \epsilon_{V_1}^*)(p_{V_1} \cdot p_{V_2} + p_{V_1}^2) - (p_1 \cdot p_{V_1})(p_1 \cdot \epsilon_{V_1}^* + p_{V_2} \cdot \epsilon_{V_1}^*)] \\
&\quad + \epsilon_{\alpha\beta\delta\lambda} p_{V_1}^\alpha p_{V_2}^\beta \epsilon_{V_1}^{\delta*} p_1^\lambda (p_1 \cdot p_{V_2})(p_1 \cdot \epsilon_{V_2}^*) \}. \tag{A15}
\end{aligned}$$

$\tilde{I}[(\text{PC}), K^*, \bar{K}^*, (K^*)]:$

$$\begin{aligned}
i\mathcal{M} &= g_1 g_2 g_3 \int \frac{d^4 p_1}{(2\pi)^4} \frac{\epsilon_{\alpha\beta\mu\nu} p_1^\alpha p_3^\beta (g^{\mu\mu'} - \frac{p_1^\mu p_1^{\mu'}}{p_1^2})(g^{\rho\sigma} - \frac{p_2^\rho p_2^\sigma}{p_2^2})(g^{\nu\nu'} - \frac{p_3^\nu p_3^{\nu'}}{p_3^2})}{(p_1^2 - m_{K^*}^2 + i\epsilon)(p_2^2 - m_{K^*}^2 + i\epsilon)(p_3^2 - m_{K^*}^2 + i\epsilon)} \\
&\quad \times [(p_1 + p_{V_1})_\rho \epsilon_{V_1}^{\delta*} g_{\mu\delta} + (p_2 - p_{V_1})_{\mu'} \epsilon_{V_1}^{\delta*} g_{\delta\rho} - (p_1 + p_2)_\delta \epsilon_{V_1}^{\delta*} g_{\mu\rho}] \\
&\quad \times [(p_3 + p_{V_2})_\sigma \epsilon_{V_2}^{\lambda*} g_{\nu\lambda} - (p_2 + p_{V_2})_{\nu'} \epsilon_{V_2}^{\lambda*} g_{\lambda\sigma} + (p_2 - p_3)_\lambda \epsilon_{V_2}^{\lambda*} g_{\nu\sigma}] \mathcal{F}(p_i^2) \\
&= g_1 g_2 g_3 \int \frac{d^4 p_1}{(2\pi)^4} \frac{\epsilon_{\alpha\beta\mu\nu} p_1^\alpha p_3^\beta (g^{\rho\sigma} - \frac{p_2^\rho p_2^\sigma}{p_2^2})}{(p_1^2 - m_{K^*}^2 + i\epsilon)(p_2^2 - m_{K^*}^2 + i\epsilon)(p_3^2 - m_{K^*}^2 + i\epsilon)} \mathcal{F}(p_i^2) \\
&\quad \times [(p_1 + p_{V_1})_\rho \epsilon_{V_1}^{\delta*} g_{\mu\delta} + (p_2 - p_{V_1})_\mu \epsilon_{V_1}^{\delta*} g_{\delta\rho} - (p_1 + p_2)_\delta \epsilon_{V_1}^{\delta*} g_{\mu\rho}] \\
&\quad \times [(p_3 + p_{V_2})_\sigma \epsilon_{V_2}^{\lambda*} g_{\nu\lambda} - (p_2 + p_{V_2})_\nu \epsilon_{V_2}^{\lambda*} g_{\lambda\sigma} + (p_2 - p_3)_\lambda \epsilon_{V_2}^{\lambda*} g_{\nu\sigma}] \\
&= g_1 g_2 g_3 \int \frac{d^4 p_1}{(2\pi)^4} \frac{4\mathcal{F}(p_i^2)}{p_2^2 (p_1^2 - m_{K^*}^2 + i\epsilon)(p_2^2 - m_{K^*}^2 + i\epsilon)(p_3^2 - m_{K^*}^2 + i\epsilon)} \\
&\quad \times \{ \epsilon_{\alpha\beta\delta\lambda} p_1^\alpha p_{V_2}^\beta \epsilon_{V_1}^{\delta*} \epsilon_{V_2}^{\lambda*} [(p_1^2 - p_1 \cdot p_{V_1})(p_{V_1} \cdot p_{V_2}) + (p_{V_1}^2 - p_1 \cdot p_{V_1})(p_1 \cdot p_{V_2})] \\
&\quad + \epsilon_{\alpha\beta\delta\lambda} p_{V_1}^\alpha p_1^\beta \epsilon_{V_1}^{\delta*} \epsilon_{V_2}^{\lambda*} [(p_1 \cdot p_{V_1} - p_1^2)(p_{V_1} \cdot p_{V_2}) + (p_1 \cdot p_{V_1} - p_{V_1}^2)(p_1 \cdot p_{V_2})] \\
&\quad + \epsilon_{\alpha\beta\delta\lambda} p_{V_1}^\alpha p_{V_2}^\beta p_1^\delta \epsilon_{V_2}^{\lambda*} p_2^2 [-2(p_1 \cdot \epsilon_{V_1}^*) + (p_{V_2} \cdot \epsilon_{V_1}^*)] \\
&\quad + \epsilon_{\alpha\beta\delta\lambda} p_{V_1}^\alpha p_{V_2}^\beta \epsilon_{V_1}^{\delta*} p_1^\lambda p_2^2 [-2(p_1 \cdot \epsilon_{V_2}^*) + (p_{V_1} \cdot \epsilon_{V_2}^*)] \}. \tag{A16}
\end{aligned}$$

$\tilde{I}[(\text{PC}), K^*, \bar{K}^*, (\kappa)]:$

$$\begin{aligned}
i\mathcal{M} &= g_1 g_2 g_3 \int \frac{d^4 p_1}{(2\pi)^4} \frac{\epsilon_{\alpha\beta\mu\nu} p_1^\alpha p_3^\beta (g^{\mu\rho} - \frac{p_1^\mu p_1^\rho}{p_1^2})(g^{\nu\sigma} - \frac{p_3^\nu p_3^\sigma}{p_3^2}) \epsilon_{V_1}^{\sigma*} \epsilon_{V_2}^{\nu*}}{(p_1^2 - m_{K^*}^2 + i\epsilon)(p_2^2 - m_K^2 + i\epsilon)(p_3^2 - m_{K^*}^2 + i\epsilon)} \mathcal{F}(p_i^2) \\
&= g_1 g_2 g_3 \int \frac{d^4 p_1}{(2\pi)^4} \frac{\epsilon_{\alpha\beta\mu\nu} p_1^\alpha p_3^\beta \epsilon_{V_1}^{\mu*} \epsilon_{V_2}^{\nu*}}{(p_1^2 - m_{K^*}^2 + i\epsilon)(p_2^2 - m_K^2 + i\epsilon)(p_3^2 - m_{K^*}^2 + i\epsilon)} \mathcal{F}(p_i^2) \\
&= g_1 g_2 g_3 \int \frac{d^4 p_1}{(2\pi)^4} \frac{\mathcal{F}(p_i^2)}{(p_1^2 - m_{K^*}^2 + i\epsilon)(p_2^2 - m_K^2 + i\epsilon)(p_3^2 - m_{K^*}^2 + i\epsilon)} \\
&\quad \times \{ \epsilon_{\alpha\beta\delta\lambda} p_1^\alpha p_{V_2}^\beta \epsilon_{V_1}^{\delta*} \epsilon_{V_2}^{\lambda*} - \epsilon_{\alpha\beta\delta\lambda} p_{V_1}^\alpha p_1^\beta \epsilon_{V_1}^{\delta*} \epsilon_{V_2}^{\lambda*} \}. \tag{A17}
\end{aligned}$$

$\tilde{\mathcal{I}}[(\text{PC}), K, \bar{K}^*, (K)]:$

$$\begin{aligned}
i\mathcal{M} &= g_1 g_2 g_3 \int \frac{d^4 p_1}{(2\pi)^4} \frac{(p_D + p_1)_\mu (p_1 + p_2)_\rho \epsilon_{\alpha\beta\nu\sigma} p_3^\alpha p_{V_2}^\beta \epsilon_{V_1}^{\rho*} \epsilon_{V_2}^{\sigma*} (g^{\mu\nu} - \frac{p_3^\mu p_3^\nu}{p_3^2})}{(p_1^2 - m_K^2 + i\epsilon)(p_2^2 - m_K^2 + i\epsilon)(p_3^2 - m_{K^*}^2 + i\epsilon)} \mathcal{F}(p_i^2) \\
&= g_1 g_2 g_3 \int \frac{d^4 p_1}{(2\pi)^4} \frac{(p_D + p_1)^\mu (p_1 + p_2)_\rho \epsilon_{\alpha\beta\mu\sigma} p_3^\alpha p_{V_2}^\beta \epsilon_{V_1}^{\rho*} \epsilon_{V_2}^{\sigma*}}{(p_1^2 - m_K^2 + i\epsilon)(p_2^2 - m_K^2 + i\epsilon)(p_3^2 - m_{K^*}^2 + i\epsilon)} \mathcal{F}(p_i^2) \\
&= g_1 g_2 g_3 \int \frac{4\mathcal{F}(p_i^2)}{(p_1^2 - m_K^2 + i\epsilon)(p_2^2 - m_K^2 + i\epsilon)(p_3^2 - m_{K^*}^2 + i\epsilon)} \\
&\quad \times \epsilon_{\alpha\beta\delta\lambda} p_{V_1}^\alpha p_{V_2}^\beta p_1^\delta \epsilon_{V_2}^\lambda (p_1 \cdot \epsilon_{V_1}^*).
\end{aligned} \tag{A18}$$

$\tilde{\mathcal{I}}[(\text{PC}), K^*, \bar{K}, (K)]:$

$$\begin{aligned}
i\mathcal{M} &= g_1 g_2 g_3 \int \frac{d^4 p_1}{(2\pi)^4} \frac{(p_D + p_3)_\mu (p_3 - p_2)_\rho \epsilon_{\alpha\beta\nu\sigma} p_1^\alpha p_{V_1}^\beta \epsilon_{V_1}^{\sigma*} \epsilon_{V_2}^{\rho*} (g^{\mu\nu} - \frac{p_1^\mu p_1^\nu}{p_1^2})}{(p_1^2 - m_{K^*}^2 + i\epsilon)(p_2^2 - m_K^2 + i\epsilon)(p_3^2 - m_K^2 + i\epsilon)} \mathcal{F}(p_i^2) \\
&= g_1 g_2 g_3 \int \frac{d^4 p_1}{(2\pi)^4} \frac{(p_D + p_3)^\mu (p_3 - p_2)_\rho \epsilon_{\alpha\beta\mu\sigma} p_1^\alpha p_{V_1}^\beta \epsilon_{V_1}^{\sigma*} \epsilon_{V_2}^{\rho*}}{(p_1^2 - m_{K^*}^2 + i\epsilon)(p_2^2 - m_K^2 + i\epsilon)(p_3^2 - m_K^2 + i\epsilon)} \mathcal{F}(p_i^2) \\
&= g_1 g_2 g_3 \int \frac{d^4 p_1}{(2\pi)^4} \frac{4\mathcal{F}(p_i^2)}{(p_1^2 - m_{K^*}^2 + i\epsilon)(p_2^2 - m_K^2 + i\epsilon)(p_3^2 - m_K^2 + i\epsilon)} \\
&\quad \times \epsilon_{\alpha\beta\delta\lambda} p_{V_1}^\alpha p_{V_2}^\beta \epsilon_{V_1}^{\delta*} p_1^\lambda (p_1 \cdot \epsilon_{V_2}^* - p_{V_1} \cdot \epsilon_{V_2}^*).
\end{aligned} \tag{A19}$$

$\tilde{\mathcal{I}}[(\text{PC}), K, \bar{K}^*, (K^*)]:$

$$\begin{aligned}
i\mathcal{M} &= g_1 g_2 g_3 \int \frac{d^4 p_1}{(2\pi)^4} \frac{(p_D + p_1)_\nu \epsilon_{\alpha\beta\rho\delta} p_2^\alpha p_{V_1}^\beta \epsilon_{V_1}^{\delta*} (g^{\mu\nu} - \frac{p_3^\mu p_3^\nu}{p_3^2}) (g^{\rho\sigma} - \frac{p_2^\rho p_2^\sigma}{p_2^2})}{(p_1^2 - m_K^2 + i\epsilon)(p_2^2 - m_{K^*}^2 + i\epsilon)(p_3^2 - m_{K^*}^2 + i\epsilon)} \\
&\quad \times [(p_3 + p_{V_2})_\sigma \epsilon_{V_2\mu}^* + (p_2 - p_3)_\lambda \epsilon_{V_2}^{\lambda*} g_{\mu\sigma} - (p_2 + p_{V_2})_\mu \epsilon_{V_2\sigma}^*] \mathcal{F}(p_i^2) \\
&= g_1 g_2 g_3 \int \frac{d^4 p_1}{(2\pi)^4} \frac{(p_D + p_1)_\nu \epsilon_{\alpha\beta\rho\delta} p_2^\alpha p_{V_1}^\beta \epsilon_{V_1}^{\delta*} (g^{\mu\nu} - \frac{p_3^\mu p_3^\nu}{p_3^2})}{(p_1^2 - m_{K^*}^2 + i\epsilon)(p_2^2 - m_K^2 + i\epsilon)(p_3^2 - m_K^2 + i\epsilon)} \\
&\quad \times [(p_3 + p_{V_2})^\rho \epsilon_{V_2\mu}^* + (p_2 - p_3)_\lambda \epsilon_{V_2}^{\lambda*} g_\mu^\rho - (p_2 + p_{V_2})_\mu \epsilon_{V_2}^{\rho*}] \mathcal{F}(p_i^2) \\
&= g_1 g_2 g_3 \int \frac{d^4 p_1}{(2\pi)^4} \frac{4\mathcal{F}(p_i^2)}{p_3^2 (p_1^2 - m_{K^*}^2 + i\epsilon)(p_2^2 - m_K^2 + i\epsilon)(p_3^2 - m_K^2 + i\epsilon)} \\
&\quad \times \{ \epsilon_{\alpha\beta\delta\lambda} p_{V_1}^\alpha p_1^\beta \epsilon_{V_1}^{\delta*} \epsilon_{V_2}^{\lambda*} [(p_1 \cdot p_{V_2})(p_{V_1}^2 + p_{V_1} \cdot p_{V_2} - p_1 \cdot p_{V_2}) + p_1^2 (p_{V_2}^2 + p_{V_1} \cdot p_{V_2}) \\
&\quad - (p_1 \cdot p_{V_1})(p_{V_2}^2 + p_{V_1} \cdot p_{V_2} + p_1 \cdot p_{V_2})] + \epsilon_{\alpha\beta\delta\lambda} p_{V_1}^\alpha p_{V_2}^\beta \epsilon_{V_1}^{\delta*} p_1^\lambda [p_3^2 (p_1 \cdot \epsilon_{V_2}^*)] \}.
\end{aligned} \tag{A20}$$

$\tilde{\mathcal{I}}[(\text{PC}), K^*, \bar{K}, (K^*)]:$

$$\begin{aligned}
i\mathcal{M} &= g_1 g_2 g_3 \int \frac{d^4 p_1}{(2\pi)^4} \frac{(p_D + p_3)_\mu \epsilon_{\alpha\beta\sigma\lambda} p_2^\alpha p_{V_2}^\beta \epsilon_{V_2}^{\lambda*} (g^{\mu\nu} - \frac{p_1^\mu p_1^\nu}{p_1^2}) (g^{\rho\sigma} - \frac{p_2^\rho p_2^\sigma}{p_2^2})}{(p_1^2 - m_{K^*}^2 + i\epsilon)(p_2^2 - m_{K^*}^2 + i\epsilon)(p_3^2 - m_K^2 + i\epsilon)} \\
&\quad \times [(p_1 + p_{V_1})_\rho \epsilon_{V_1}^{\rho*} + (p_2 - p_{V_1})_\nu \epsilon_{V_1}^{\nu*} - (p_1 + p_2)_\delta \epsilon_{V_1}^{\delta*} g_{\nu\rho}] \mathcal{F}(p_i^2) \\
&= g_1 g_2 g_3 \int \frac{d^4 p_1}{(2\pi)^4} \frac{(p_D + p_3)_\mu \epsilon_{\alpha\beta\sigma\lambda} p_2^\alpha p_{V_2}^\beta \epsilon_{V_2}^{\lambda*} (g^{\mu\nu} - \frac{p_1^\mu p_1^\nu}{p_1^2})}{(p_1^2 - m_{K^*}^2 + i\epsilon)(p_2^2 - m_{K^*}^2 + i\epsilon)(p_3^2 - m_K^2 + i\epsilon)} \\
&\quad \times [(p_1 + p_{V_1})^\sigma \epsilon_{V_1}^{\sigma*} + (p_2 - p_{V_1})_\nu \epsilon_{V_1}^{\nu*} - (p_1 + p_2)_\delta \epsilon_{V_1}^{\delta*} g_\nu^\sigma] \mathcal{F}(p_i^2) \\
&= g_1 g_2 g_3 \int \frac{d^4 p_1}{(2\pi)^4} \frac{4\mathcal{F}(p_i^2)}{p_1^2 (p_1^2 - m_{K^*}^2 + i\epsilon)(p_2^2 - m_{K^*}^2 + i\epsilon)(p_3^2 - m_K^2 + i\epsilon)} \\
&\quad \times \{ \epsilon_{\alpha\beta\delta\lambda} p_{V_1}^\alpha p_{V_2}^\beta \epsilon_{V_1}^{\delta*} \epsilon_{V_2}^{\lambda*} [(p_1 \cdot p_{V_1})^2 + (p_1 \cdot p_{V_1})(p_1 \cdot p_{V_2}) - p_1^2 (p_{V_1}^2 + p_{V_1} \cdot p_{V_2})] \\
&\quad + \epsilon_{\alpha\beta\delta\lambda} p_1^\alpha p_{V_2}^\beta \epsilon_{V_1}^{\delta*} \epsilon_{V_2}^{\lambda*} [-(p_1 \cdot p_{V_1})^2 - (p_1 \cdot p_{V_1})(p_1 \cdot p_{V_2}) + p_1^2 (p_{V_1}^2 + p_{V_1} \cdot p_{V_2})] \\
&\quad + \epsilon_{\alpha\beta\delta\lambda} p_{V_1}^\alpha p_{V_2}^\beta p_1^\delta \epsilon_{V_2}^{\lambda*} [(p_{V_2} \cdot \epsilon_{V_1}^* - p_1 \cdot \epsilon_{V_1}^*) p_1^\lambda] \}. \tag{A21}
\end{aligned}$$

$\tilde{\mathcal{I}}[(\text{PV}), K^*, \bar{K}^*, (K)]:$

$$\begin{aligned}
i\mathcal{M} &= g_1 g_2 g_3 \int \frac{d^4 p_1}{(2\pi)^4} \frac{\epsilon_{\alpha_1\beta_1\mu\delta} p_1^{\alpha_1} p_{V_1}^{\beta_1} \epsilon_{V_1}^{\delta*} (g^{\mu\rho} - \frac{p_1^\mu p_1^\rho}{p_1^2}) \epsilon^{\alpha_2\beta_2\nu\lambda} p_{3\alpha_2} p_{V_2\beta_2} \epsilon_{\phi\lambda}^* (g_{\nu\rho} - \frac{p_{3\nu} p_{3\rho}}{p_3^2})}{(p_1^2 - m_{K^*}^2 + i\epsilon)(p_2^2 - m_K^2 + i\epsilon)(p_3^2 - m_{K^*}^2 + i\epsilon)} \mathcal{F}(p_i^2) \\
&= g_1 g_2 g_3 \int \frac{d^4 p_1}{(2\pi)^4} \frac{\epsilon_{\alpha_1\beta_1\mu\delta} p_1^{\alpha_1} p_{V_1}^{\beta_1} \epsilon_{V_1}^{\delta*} \times \epsilon^{\alpha_2\beta_2\mu\lambda} p_{3\alpha_2} p_{V_2\beta_2} \epsilon_{V_2\lambda}^*}{(p_1^2 - m_{K^*}^2 + i\epsilon)(p_2^2 - m_K^2 + i\epsilon)(p_3^2 - m_{K^*}^2 + i\epsilon)} \mathcal{F}(p_i^2) \\
&= g_1 g_2 g_3 \int \frac{d^4 p_1}{(2\pi)^4} \frac{\mathcal{F}(p_i^2)}{(p_1^2 - m_{K^*}^2 + i\epsilon)(p_2^2 - m_K^2 + i\epsilon)(p_3^2 - m_{K^*}^2 + i\epsilon)} \\
&\quad \times \{ (\epsilon_{V_1}^* \cdot \epsilon_{V_2}^*) [(p_1^2 - p_1 \cdot p_{V_1})(p_{V_1} \cdot p_{V_2}) + (p_{V_1}^2 - p_1 \cdot p_{V_1})(p_1 \cdot p_{V_2})] \\
&\quad - (p_1 \cdot \epsilon_{V_1}^*)(p_1 \cdot \epsilon_{V_2}^*)(p_{V_1} \cdot p_{V_2}) + (p_1 \cdot \epsilon_{V_1}^*)(p_{V_1} \cdot \epsilon_{V_2}^*)(p_1 \cdot p_{V_2}) \\
&\quad + (p_{V_2} \cdot \epsilon_{V_1}^*)(p_1 \cdot \epsilon_{V_2}^*) [(p_1 \cdot p_{V_1}) - p_{V_1}^2] \\
&\quad + (p_{V_2} \cdot \epsilon_{V_1}^*)(p_{V_1} \cdot \epsilon_{V_2}^*) [(p_1 \cdot p_{V_1}) - p_{V_1}^2] \}. \tag{A22}
\end{aligned}$$

$\tilde{\mathcal{I}}[(\text{PV}), K^*, \bar{K}^*, (K^*)]:$

$$\begin{aligned}
i\mathcal{M} &= g_1 g_2 g_3 \int \frac{d^4 p_1}{(2\pi)^4} \frac{(g^{\mu\lambda} - \frac{p_1^\mu p_1^\lambda}{p_1^2}) (g^{\rho\sigma} - \frac{p_2^\rho p_2^\sigma}{p_2^2}) (g_{\nu\lambda} - \frac{p_{3\nu} p_{3\lambda}}{p_3^2})}{(p_1^2 - m_{K^*}^2 + i\epsilon)(p_2^2 - m_{K^*}^2 + i\epsilon)(p_3^2 - m_{K^*}^2 + i\epsilon)} \\
&\quad \times [(p_1 + p_{V_1})_\rho \epsilon_{V_1}^{\rho*} g_{\mu\delta} + (p_2 - p_{V_1})_\mu \epsilon_{V_1}^{\mu*} g_{\delta\rho} - (p_1 + p_2)_\delta \epsilon_{V_1}^{\delta*} g_{\mu\rho}] \\
&\quad \times [(p_3 + p_{V_2})_\sigma \epsilon_{V_2\beta}^* g^{\nu\beta} - (p_2 + p_{V_2})^\nu \epsilon_{V_2}^{\beta*} g_{\beta\sigma} + (p_2 - p_3)_\beta \epsilon_{V_2}^{\beta*} g_\sigma^\nu] \mathcal{F}(p_i^2) \\
&= g_1 g_2 g_3 \int \frac{d^4 p_1}{(2\pi)^4} \frac{(p_1^2 g^{\mu\lambda} - p_1^\mu p_1^\lambda) (p_2^2 g^{\rho\sigma} - p_2^\rho p_2^\sigma) (p_3^2 g_{\nu\lambda} - p_{3\nu} p_{3\lambda})}{p_1^2 p_2^2 p_3^2 (p_1^2 - m_{K^*}^2 + i\epsilon)(p_2^2 - m_{K^*}^2 + i\epsilon)(p_3^2 - m_{K^*}^2 + i\epsilon)} \\
&\quad \times [(p_1 + p_{V_1})_\rho \epsilon_{V_1}^{\rho*} g_{\mu\delta} + (p_2 - p_{V_1})_\mu \epsilon_{V_1}^{\mu*} g_{\delta\rho} - (p_1 + p_2)_\delta \epsilon_{V_1}^{\delta*} g_{\mu\rho}] \\
&\quad \times [(p_3 + p_{V_2})_\sigma \epsilon_{V_2\beta}^* g^{\nu\beta} - (p_2 + p_{V_2})^\nu \epsilon_{V_2}^{\beta*} g_{\beta\sigma} + (p_2 - p_3)_\beta \epsilon_{V_2}^{\beta*} g_\sigma^\nu] \mathcal{F}(p_i^2). \tag{A23}
\end{aligned}$$

$\tilde{\mathcal{I}}[(PV), K^*, \bar{K}^*, (\kappa)]:$

$$\begin{aligned}
i\mathcal{M} &= g_1 g_2 g_3 \int \frac{d^4 p_1}{(2\pi)^4} \frac{(g^{\mu\rho} - \frac{p_1^\mu p_1^\rho}{p_1^2})(g_{\mu\sigma} - \frac{p_{3\mu} p_{3\sigma}}{p_3^2}) \epsilon_{V_1\rho}^* \epsilon_{V_2}^{\sigma*}}{(p_1^2 - m_{K^*}^2 + i\epsilon)(p_2^2 - m_K^2 + i\epsilon)(p_3^2 - m_{K^*}^2 + i\epsilon)} \mathcal{F}(p_i^2) \\
&= g_1 g_2 g_3 \int \frac{d^4 p_1}{(2\pi)^4} \frac{(p_1^\mu g^{\mu\rho} - p_1^\mu p_1^\rho)(p_3^\nu g_{\nu\sigma} - p_{3\nu} p_{3\sigma}) \epsilon_{V_1\rho}^* \epsilon_{V_2}^{\sigma*}}{p_1^2 p_3^2 (p_1^2 - m_{K^*}^2 + i\epsilon)(p_2^2 - m_K^2 + i\epsilon)(p_3^2 - m_{K^*}^2 + i\epsilon)} \mathcal{F}(p_i^2) \\
&= g_1 g_2 g_3 \int \frac{d^4 p_1}{(2\pi)^4} \frac{\mathcal{F}(p_i^2)}{p_1^2 p_3^2 (p_1^2 - m_{K^*}^2 + i\epsilon)(p_2^2 - m_K^2 + i\epsilon)(p_3^2 - m_{K^*}^2 + i\epsilon)} \\
&\quad \times \{(\epsilon_{V_1}^* \cdot \epsilon_{V_2}^*) p_1^2 p_3^2 + (p_1 \cdot \epsilon_{V_1}^*)(p_1 \cdot \epsilon_{V_2}^*)[(p_1 \cdot p_3) - (p_{V_1} + p_{V_2})^2] \\
&\quad + (p_1 \cdot \epsilon_{V_1})(p_{V_1} \cdot \epsilon_{V_2})[p_1 \cdot (p_{V_1} + p_{V_2})] + (p_{V_2} \cdot \epsilon_{V_1})(p_1 \cdot \epsilon_{V_2}) p_1^2 \\
&\quad - (p_{V_2} \cdot \epsilon_{V_1})(p_{V_1} \cdot \epsilon_{V_2}) p_1^2\}.
\end{aligned} \tag{A24}$$

$\tilde{\mathcal{I}}[(PV), K, \bar{K}, (K)]:$

$$\begin{aligned}
i\mathcal{M} &= g_1 g_2 g_3 \int \frac{d^4 p_1}{(2\pi)^4} \frac{(p_1 + p_2)_\mu (p_2 - p_3)_\nu \epsilon_{V_1}^{\mu*} \epsilon_{V_2}^{\nu*}}{(p_1^2 - m_K^2 + i\epsilon)(p_2^2 - m_K^2 + i\epsilon)(p_3^2 - m_K^2 + i\epsilon)} \mathcal{F}(p_i^2) \\
&= g_1 g_2 g_3 \int \frac{d^4 p_1}{(2\pi)^4} \frac{4\mathcal{F}(p_i^2)}{(p_1^2 - m_K^2 + i\epsilon)(p_2^2 - m_K^2 + i\epsilon)(p_3^2 - m_K^2 + i\epsilon)} \\
&\quad \times (p_1 \cdot \epsilon_{V_1}^*)(p_1 \cdot \epsilon_{V_2}^* - p_{V_1} \cdot \epsilon_{V_2}^*).
\end{aligned} \tag{A25}$$

$\tilde{\mathcal{I}}[PV, K, \bar{K}, (K^*)]:$

$$\begin{aligned}
i\mathcal{M} &= g_1 g_2 g_3 \int \frac{d^4 p_1}{(2\pi)^4} \frac{\epsilon_{\alpha\beta\mu\lambda} p_2^\alpha p_{V_1}^\beta \epsilon_{V_1}^{\lambda*} \epsilon_{\alpha_1\beta_1\nu\delta} p_2^{\alpha_1} p_{V_2}^{\beta_1} \epsilon_{V_2}^{\delta*} (g^{\mu\nu} - \frac{p_2^\mu p_2^\nu}{p_2^2})}{(p_1^2 - m_K^2 + i\epsilon)(p_2^2 - m_{K^*}^2 + i\epsilon)(p_3^2 - m_K^2 + i\epsilon)} \mathcal{F}(p_i^2) \\
&= g_1 g_2 g_3 \int \frac{d^4 p_1}{(2\pi)^4} \frac{\epsilon_{\alpha\beta\mu\lambda} p_2^\alpha p_{V_1}^\beta \epsilon_{V_1}^{\lambda*} \epsilon_{\alpha_1\beta_1\nu\delta} p_2^{\alpha_1} p_{V_2}^{\beta_1} \epsilon_{V_2}^{\delta*}}{(p_1^2 - m_K^2 + i\epsilon)(p_2^2 - m_{K^*}^2 + i\epsilon)(p_3^2 - m_K^2 + i\epsilon)} \mathcal{F}(p_i^2) \\
&= g_1 g_2 g_3 \int \frac{d^4 p_1}{(2\pi)^4} \frac{\mathcal{F}(p_i^2)}{(p_1^2 - m_K^2 + i\epsilon)(p_2^2 - m_{K^*}^2 + i\epsilon)(p_3^2 - m_K^2 + i\epsilon)} \\
&\quad \times \{(\epsilon_{V_1}^* \cdot \epsilon_{V_2}^*)[(p_1 \cdot p_{V_2})(p_1 \cdot p_{V_1} - p_{V_1}^2) + (p_{V_1} \cdot p_{V_2})(p_1 \cdot p_{V_1} - p_1^2)] \\
&\quad + (p_1 \cdot \epsilon_{V_1}^*)(p_1 \cdot \epsilon_{V_2}^*)(p_{V_1} \cdot p_{V_2}) - (p_1 \cdot \epsilon_{V_1}^*)(p_{V_1} \cdot \epsilon_{V_2}^*)(p_{V_1} \cdot p_{V_2}) \\
&\quad + (p_{V_2} \cdot \epsilon_{V_1}^*)(p_1 \cdot \epsilon_{V_2}^*)[p_{V_1}^2 - (p_1 \cdot p_{V_1})] \\
&\quad + (p_{V_2} \cdot \epsilon_{V_1}^*)(p_{V_1} \cdot \epsilon_{V_2}^*)[p_1^2 - (p_1 \cdot p_{V_1})]\}.
\end{aligned} \tag{A26}$$

In the above amplitudes, the product of the propagators and the form factor can be expanded as

$$\begin{aligned}
\frac{\mathcal{F}(q_i^2)}{D_1 D_2 D_3} &= \frac{1}{(p_1^2 - m_1^2)(p_2^2 - m_2^2)(p_3^2 - m_3^2)} \left(\frac{m_1^2 - \Lambda_1^2}{p_1^2 - \Lambda_1^2} \right) \left(\frac{m_2^2 - \Lambda_2^2}{p_2^2 - \Lambda_2^2} \right) \left(\frac{m_3^2 - \Lambda_3^2}{p_3^2 - \Lambda_3^2} \right) \\
&= \left(\frac{1}{p_1^2 - m_1^2} - \frac{1}{p_1^2 - \Lambda_1^2} \right) \left(\frac{1}{p_2^2 - m_2^2} - \frac{1}{p_2^2 - \Lambda_2^2} \right) \left(\frac{1}{p_3^2 - m_3^2} - \frac{1}{p_3^2 - \Lambda_3^2} \right) \\
&= \frac{1}{(p_1^2 - m_1^2)(p_2^2 - m_2^2)(p_3^2 - m_3^2)} - \frac{1}{(p_1^2 - \Lambda_1^2)(p_2^2 - m_2^2)(p_3^2 - m_3^2)} - \frac{1}{(p_1^2 - m_1^2)(p_2^2 - \Lambda_2^2)(p_3^2 - m_3^2)} \\
&\quad - \frac{1}{(p_1^2 - m_1^2)(p_2^2 - m_2^2)(p_3^2 - \Lambda_3^2)} + \frac{1}{(p_1^2 - \Lambda_1^2)(p_2^2 - \Lambda_2^2)(p_3^2 - m_3^2)} + \frac{1}{(p_1^2 - \Lambda_1^2)(p_2^2 - m_2^2)(p_3^2 - \Lambda_3^2)} \\
&\quad + \frac{1}{(p_1^2 - m_1^2)(p_2^2 - \Lambda_2^2)(p_3^2 - \Lambda_3^2)} - \frac{1}{(p_1^2 - \Lambda_1^2)(p_2^2 - \Lambda_2^2)(p_3^2 - \Lambda_3^2)}.
\end{aligned} \tag{A27}$$

- [1] Bernard Aubert *et al.*, Rates, polarizations, and asymmetries in charmless vector-vector B meson decays, *Phys. Rev. Lett.* **91**, 171802 (2003).
- [2] Bernard Aubert *et al.*, Observation of the decay $B^0 \rightarrow \rho^+ \rho^-$ and measurement of the branching fraction and polarization, *Phys. Rev. D* **69**, 031102 (2004).
- [3] J. Zhang *et al.*, Observation of $B^\mp \rightarrow \rho^\mp \rho^0$, *Phys. Rev. Lett.* **91**, 221801 (2003).
- [4] Stanley J. Brodsky and G. Peter Lepage, Helicity selection rules and tests of gluon spin in exclusive QCD processes, *Phys. Rev. D* **24**, 2848 (1981).
- [5] V. L. Chernyak and A. R. Zhitnitsky, Exclusive decays of heavy mesons, *Nucl. Phys.* **B201**, 492 (1982); **B214**, 547(E) (1983).
- [6] V. L. Chernyak and A. R. Zhitnitsky, Asymptotic behavior of exclusive processes in QCD, *Phys. Rep.* **112**, 173 (1984).
- [7] K. F. Chen *et al.*, Measurement of branching fractions and polarization in $B \rightarrow \phi K^{(*)}$ decays, *Phys. Rev. Lett.* **91**, 201801 (2003).
- [8] A. N. Kamal, R. C. Verma, and N. Sinha, $(D, D_s^+) \rightarrow VV$ decays in two models: An SU(3) symmetry model and a factorization model with final state interactions, *Phys. Rev. D* **43**, 843 (1991).
- [9] Ian Hinchliffe and Thomas A. Kaeding, Nonleptonic two-body decays of D mesons in broken SU(3), *Phys. Rev. D* **54**, 914 (1996).
- [10] Paulo F. Bedaque, Ashok K. Das, and V. S. Mathur, Two-body nonleptonic decays of charmed mesons, *Phys. Rev. D* **49**, 269 (1994).
- [11] Manfred Bauer, B. Stech, and M. Wirbel, Exclusive nonleptonic decays of D , D_s , and B mesons, *Z. Phys. C* **34**, 103 (1987).
- [12] Hai-Yang Cheng and Cheng-Wei Chiang, Long-distance contributions to $D^0 - \bar{D}^0$ mixing parameters, *Phys. Rev. D* **81**, 114020 (2010).
- [13] Hua-Yu Jiang, Fu-Sheng Yu, Qin Qin, Hsiang-nan Li, and Cai-Dian Lü, $D^0 - \bar{D}^0$ mixing parameter γ in the factorization-assisted topological-amplitude approach, *Chin. Phys. C* **42**, 063101 (2018).
- [14] T. Uppal and R. C. Verma, Branching ratios for $D \rightarrow VV$ decays in presence of smearing effects due to ρ meson width, *Z. Phys. C* **56**, 273 (1992).
- [15] B. Bajc, S. Fajfer, R. J. Oakes, and Sasa Prelovsek, Nonleptonic two-body charmed meson decays in an effective model for their semileptonic decays, *Phys. Rev. D* **56**, 7207 (1997).
- [16] El Hassan El Aaoud and A. N. Kamal, Helicity and partial wave amplitude analysis of $D \rightarrow K * \rho$ decay, *Phys. Rev. D* **59**, 114013 (1999).
- [17] Gudrun Hiller and Roman Zwicky, (A)symmetries of weak decays at and near the kinematic endpoint, *J. High Energy Phys.* **03** (2014) 042.
- [18] D. Coffman *et al.*, Resonant substructure in $\bar{K} \pi \pi \pi$ decays of D mesons, *Phys. Rev. D* **45**, 2196 (1992).
- [19] J. M. Link *et al.*, Study of the $D^0 \rightarrow \pi^- \pi^+ \pi^- \pi^+$ decay, *Phys. Rev. D* **75**, 052003 (2007).
- [20] M. Ablikim *et al.*, First measurement of polarizations in the decay $D^0 \rightarrow \omega \phi$, *Phys. Rev. Lett.* **128**, 011803 (2022).
- [21] Philippe d'Argent, Nicola Skidmore, Jack Benton, Jeremy Dalseno, Evelina Gersabeck, Sam Harnew, Paras Naik, Claire Prouve, and Jonas Rademacker, Amplitude analyses of $D^0 \rightarrow \pi^+ \pi^- \pi^+ \pi^-$ and $D^0 \rightarrow K^+ K^- \pi^+ \pi^-$ decays, *J. High Energy Phys.* **05** (2017) 143.
- [22] Roel Aaij *et al.*, Search for CP violation through an amplitude analysis of $D^0 \rightarrow K^+ K^- \pi^+ \pi^-$ decays, *J. High Energy Phys.* **02** (2019) 126.
- [23] A. Le Yaouanc, L. Oliver, O. Pene, and J. C. Raynal, *Hadron Transitions in the Quark Model* (Gordon and Breach Science Publishers, New York, 1988).
- [24] Jean-Marc Richard, Qian Wang, and Qiang Zhao, Understanding the shortened lifetime of Λ_c^+ , [arXiv:1604.04208](https://arxiv.org/abs/1604.04208).
- [25] Peng-Yu Niu, Jean-Marc Richard, Qian Wang, and Qiang Zhao, Hadronic weak decays of Λ_c in the quark model, *Phys. Rev. D* **102**, 073005 (2020).
- [26] Richard Kokoski and Nathan Isgur, Meson decays by flux tube breaking, *Phys. Rev. D* **35**, 907 (1987).
- [27] S. Godfrey and Nathan Isgur, Mesons in a relativized quark model with chromodynamics, *Phys. Rev. D* **32**, 189 (1985).
- [28] Stephen Godfrey and Richard Kokoski, The properties of p wave mesons with one heavy quark, *Phys. Rev. D* **43**, 1679 (1991).
- [29] Peng-Yu Niu, Qian Wang, and Qiang Zhao, Study of heavy quark conserving weak decays in the quark model, *Phys. Lett. B* **826**, 136916 (2022).
- [30] Yin Cheng and Qiang Zhao, Hadronic loop effects on the radiative decays of the first radial excitations of η and η' , *Phys. Rev. D* **105**, 076023 (2022).
- [31] Yin Cheng, Lin Qiu, and Qiang Zhao, On the widths of $\eta(1295)$ and $\eta(1405/1475)$, [arXiv:2302.01210](https://arxiv.org/abs/2302.01210).
- [32] Feng-Kun Guo, Christoph Hanhart, Gang Li, Ulf-G. Meissner, and Qiang Zhao, Effect of charmed meson loops on charmonium transitions, *Phys. Rev. D* **83**, 034013 (2011).
- [33] H. Albrecht *et al.*, New results on D^0 decays, *Z. Phys. C* **56**, 7 (1992).
- [34] Medina Ablikim *et al.*, Amplitude analysis of $D^0 \rightarrow K^- \pi^+ \pi^+ \pi^-$, *Phys. Rev. D* **95**, 072010 (2017).